Arabian Journal of Chemistry (2014) 7, 347–354

King Saud University

Arabian Journal of Chemistry

www.ksu.edu.sa
www.sciencedirect.com

ORIGINAL ARTICLE

Activated carbon derived from marine Posidonia Oceanica for electric energy storage

N. Boukmouche [a,*], N. Azzouz [a], L. Bouchama [a], J.P. Chopart [b], Y. Bouznit [c]

[a] Laboratory of The Interactions Materials-Environment, Jijel University, Jijel 18000, Algeria
[b] Materials Science and Engineering Laboratory (LISM) – EA 4695, University of Reims Champagne-Ardenne, France
[c] Laboratory of Materials Study, Jijel University, Jijel 18000, Algeria

Received 6 August 2011; accepted 3 December 2012
Available online 22 December 2012

KEYWORDS
Activated carbon;
Supercapacitors;
Electric energy storage;
Electrochemical double layer

Abstract In this paper, the synthesis and characterization of activated carbon from marine Posidonia Oceanica were studied. The activated carbon was prepared by a simple process namely pyrolysis under inert atmosphere. The activated carbon can be used as electrodes for supercapacitor devices. X-ray diffraction result revealed a polycrystalline graphitic structure. While scanning electron microscope investigation showed a layered structure with micropores. The EDS analysis showed that the activated carbon contains the carbon element in high atomic percentage. Electrochemical impedance spectroscopy revealed a capacitive behavior (electrostatic phenomena). The specific capacity per unit area of the electrochemical double layer of activated carbon electrode in sulfuric acid electrolyte was 3.16 F cm^{-2}. Cyclic voltammetry and galvanostatic chronopotentiometry demonstrated that the electrode has excellent electrochemical reversibility. It has been found that the surface capacitance was strongly related to the specific surface area and pore size.

1. Introduction

Carbon materials have played important roles for the generation and storage of energy in different forms involving: activated carbon, activated carbon fiber, carbon aerogel and carbon nanotube (Inagaki et al., 2010; Zhao et al., 2007). Electrochemical capacitors, an important energy storage device, offer ideally high power density, excellent reversibility and long cycle life for time-dependent power needs of modern electronics and power systems (Huang et al., 2006; Stimpfling and Leroux, 2010; Kötz and Carlen, 2000). Electrochemical capacitors can be classified into two types according to the mechanism of energy storage; electrochemical double-layer capacitors (EDLCs) and pseudocapacitors (Burke, 2000). The capacitance of electrochemical double-layer capacitors charge is separated across the interface between electrode and electrolyte (Conway, 1999), with high surface area materials as illustrated in Fig. 1. By contrast, pseudocapacitance arises from fast and reversible redox reactions of electroactive materials with several oxidation states (metal oxides and conducting polymers) (Zheng, 1999).

Electric energy storage in electrochemical capacitors occurs due to the formation of an electric double-layer (EDL) on the

* Corresponding author. Tel.: +213 778828562.
E-mail address: nawboukmouche@yahoo.com (N. Boukmouche).
Peer review under responsibility of King Saud University.

Production and hosting by Elsevier

1878-5352 © 2012 Production and hosting by Elsevier B.V. on behalf of King Saud University.
http://dx.doi.org/10.1016/j.arabjc.2012.12.010

Nomenclature

C_S	surface capacitance (F cm^{-2})	S_{BET}	specific surface of BET (m^2 g^{-1})
f_{max}	maximum frequency (kHz)	U	overtension (V)
f_{min}	minimum frequency (kHz)	v	scan rate (mVs^{-1})

surfaces of both negative and positive charged electrodes and on some surface oxidation/reduction. Since porous carbons used for the electrodes have some amount of oxygen and/or nitrogen containing functional groups on their surfaces, there is more or less a contribution of pseudo-capacitance to the observed capacitance, so the electrochemical capacitor is called "supercapacitor" (Inagaki et al., 2010).

Posidonia Oceanica (PO) is an endemic species in the Mediterranean Sea, which like terrestrial plants, loses its leaves seasonally. The dead leaves are accumulated on the beaches in huge quantities as waste material (Balestri et al., 2006), causing great environmental and economical problems (Lafabrie et al., 2007). The dead biomass offers an abundant, renewable and low cost precursor for the production of activated carbon (ACPO) (Dural et al., 2010; Cocozza et al., 2010). In a recent study, Posidonia Oceanica has been used for the preparation of activated carbon for chemical activation with zinc chloride followed by carbonization in nitrogen atmosphere (pyrolysis) (Dural et al., 2010), where they used methylene blue adsorption. The activated carbon obtained by pyrolysis of sodium alginate has a low specific surface area. Despite that, they have a high specific capacity in the sulfuric acid medium, which demonstrates the existence of a significant contribution of pseudo-capacitive behavior (Raymundo-Piñero et al., 2006).

To our knowledge, Posidonia Oceanica was not studied so far as an activated carbon precursor like electrode material for supercapacitor for electric energy storage. In this paper, we attempt to valorize such renewable, low cost, easily available and highly abundant marine biomass for the production of the activated carbon by simple carbonization under inert atmosphere.

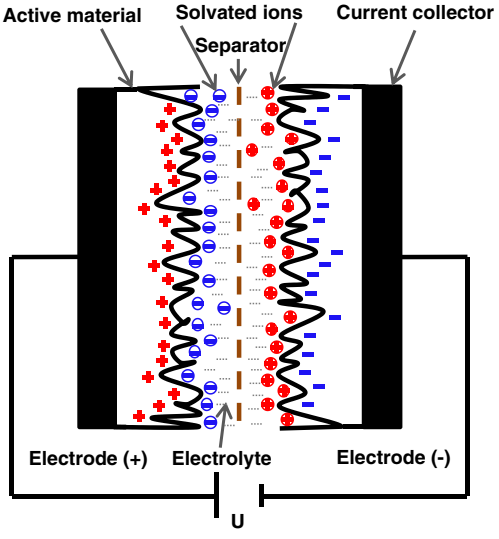

Figure 1 Sketch of the electrochemical double layer capacitor.

2. Experimental

The Posidonia Oceanica matter was abundantly washed with distilled water, then dried at 105 °C during 24 h. After its carbonization at 400 °C for three hours in the furnace under nitrogen inert atmosphere, the obtained material is then transformed into pulverized coal black color. The retained grains are chemically pretreated by phosphoric acid (H_3PO_4 1 M, 40% weight) and coal (60% weight). The reactant mixture is maintained during two hours under agitation at the ambient temperature, followed by drying of the activated carbon during 24 h at 100 °C. The product is then placed at 170 °C during 90 min. For the elimination of H_3PO_4 traces remaining in the pretreated carbon, we washed this with distilled water followed by drying during 12 h at 100 °C (Aravindhan et al., 2009; Hazourli et al., 2007). This operation is finished by grinding to obtain the powder which constitutes our working samples after the pyrolysis treatment. The last step is pyrolysis under nitrogen inert atmosphere at 600 °C under controlled heating rate of 10 °C/min to the final temperature and held at the desired temperature for 3 h. This operation enabled us to obtain a very porous activated carbon with the specific surface that we want to determine. We carried out degasification under a secondary vacuum of 10^{-7} Torr during 24 h at ambient temperature by means of EDWARDS AUTO 306 vacuum apparatus. We used a press to get our samples in the form of pellets (95% activated carbon (ACPO), 3% graphite and 2% polytetrafluoroethylene PTFE), the pressure used is 12 t (tons) at the ambient temperature and we used silver as a current collector.

The crystalline structure was analyzed by X-ray diffraction (XRD) using Cu Ka radiation (1.5418 Å) of a Bruker D8 Advance diffractometer operating at 40 kV, 40 mA for angles between 2θ = 4–90° in 0.02° steps.

The morphology of the samples was observed using a JEOL JSM 5400LV scanning electron microscope (SEM). The chemical composition of the samples has been determined by a Energy Dispersive Spectroscopy (EDS) of the emitted X-rays in a Quanta 200 instrument Scanning Electron Microscope (detector SUTW-SAPPHIRE, resolution: 135.25).

The specific surface was obtained by the adsorption isotherm measurements (BET method) employing a TriStar II 3020 V1.01 at nitrogen liquefaction temperature (77.35 K). The pore size distribution was determined by Barrett–Joiner–Halenda (BJH) and Dollimore–Heal (DH) methods.

The electrochemical measurements (cyclic voltammetry, galvanostatic charge–discharge and impedance spectroscopy) were carried out using a Voltalab 40 PGZ301 potentiostat/galvanostat of Radiometer Analytical. Voltamaster 4 software has been used for the data acquisition. The electrodes' ACPO was tested electrochemically in a three electrode cell with a 1 mol L^{-1} H_2SO_4 aqueous solution as electrolyte. The surface of the working electrode (ACPO) was 1 cm^2, the

counter-electrode was the platinum and the reference electrode was a saturated calomel electrode (SCE).

3. Result and discussion

3.1. Structural analysis

Fig. 2 shows the XRD diffractogram of the ACPO treated at different steps. PO carbonized at 400° is shown in Fig. 2a. Fig. 2b shows an XRD diagram of coal chemically activated by phosphoric acid at 170 °C, where the material is still amorphous or poorly crystallized.

The ACPO obtained in the neutral medium (N_2) at 600 °C is better crystallized with the presence of an amorphous part as seen in Fig. 3c. The structure can be assigned to that of the graphite phase with hexagonal structure (JCPDS no. 7440-44-0).

3.2. Morphological analysis

Scanning electron microscope images show a much developed porosity on all the surface of the ACPO (Fig. 3a,b). We observe that the obtained microstructure is a flat sheet like-structure. Each layer contains micropores, which were modeled in Fig. 3c.

3.3. Elemental analysis

The EDS microanalysis (Fig. 4) of Posidonia Oceanica illustrates that for the marine precursor, the carbon content C is 59.85% and the oxygen O is 25.85%. Other elements (N, Mg, S, Ag, Si, Al, K, Ti, Fe and Cu contents) were present in various percentages. This might enhance the chemical characteristics of the activated carbon by forming various functional groups. The obtained O/C ratio was 0.43; it is less than that reported by Ncibi et al. (Ncibi et al., 2009). They have obtained a ratio of 0.82. The difference can lead to the carbonization process.

3.4. Specific surface analysis

The characterization by adsorption and desorption of nitrogen allows us to determine the specific surface and the distribution of the pore size.

The reversible character shown on Fig. 5a indicates an isotherm of IIb (IUPAC) type. Thus our activated carbon

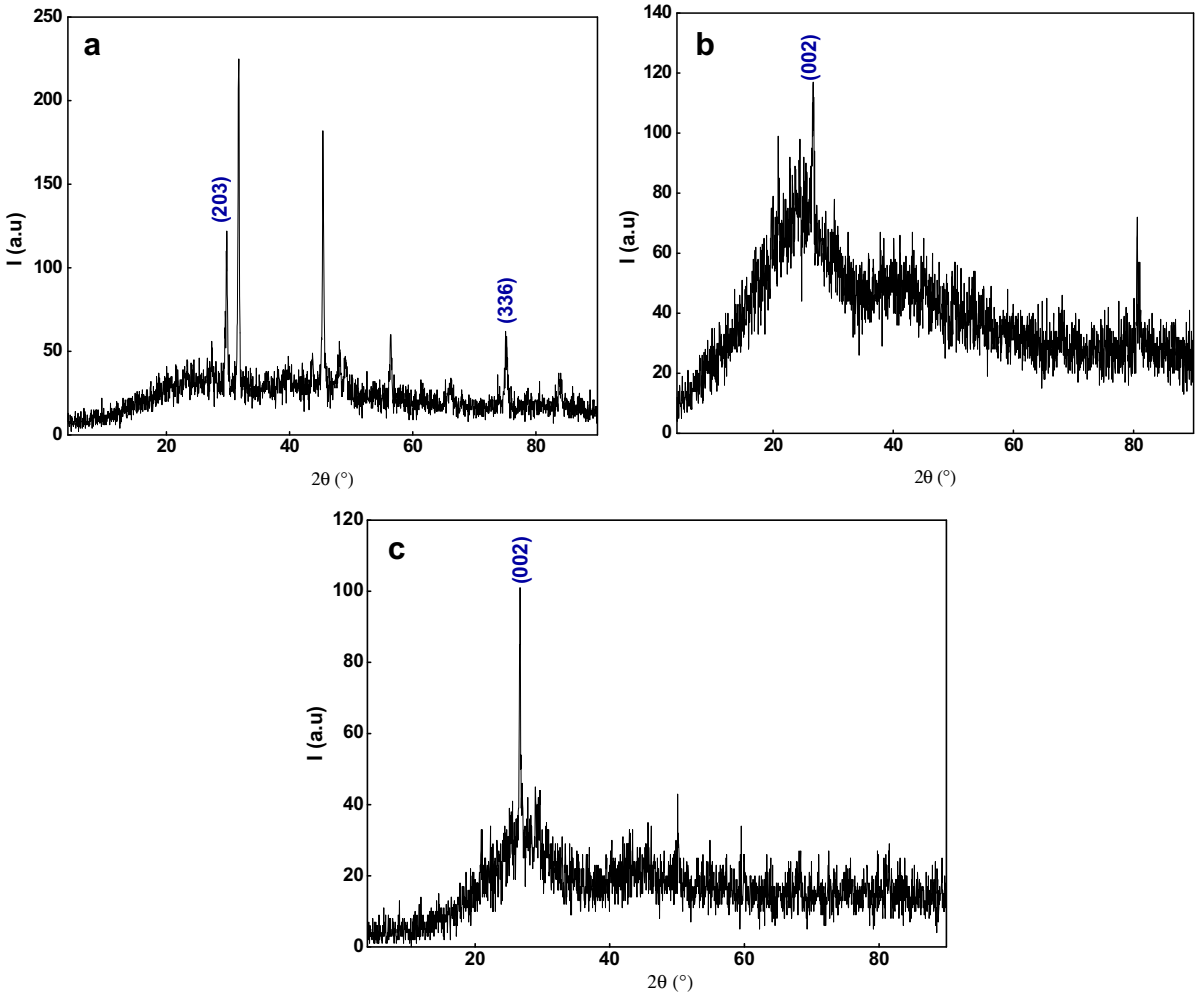

Figure 2 XRD diffractogram of ACPO: (a) coal obtained at 400 °C, (b) coal chemically activated by the phosphoric acid at 170 °C, (c) activated carbon pyrolyzed at 600 °C.

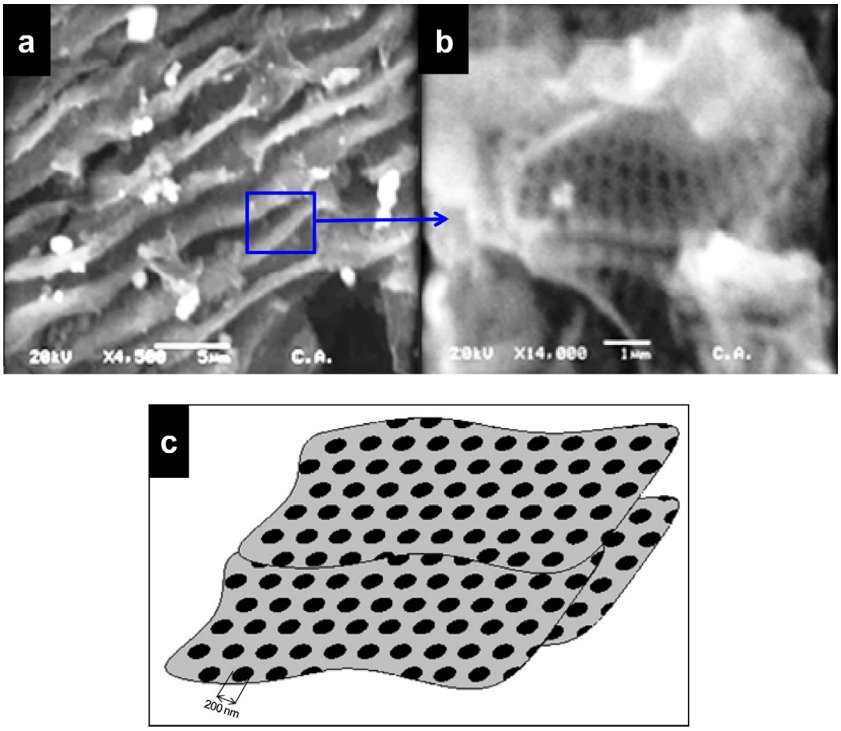

Figure 3 (a,b) SEM image of the activated carbon, (c) modeled structure.

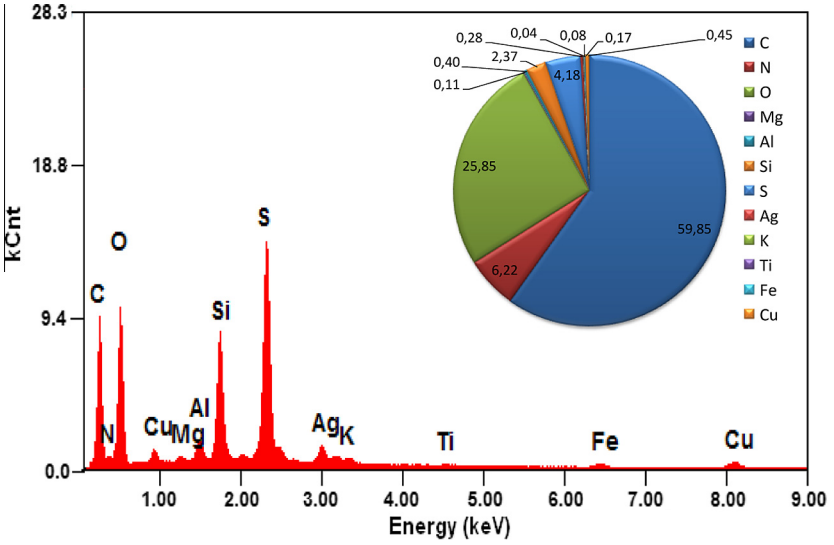

Figure 4 EDS microanalysis of the activated carbon.

contains aggregates of particles in flat sheets that have pores of nonuniform shaped slot. This hysteresis loop is observed for microporous solids (Rouquerol et al., 1999), and (Fig. 5b) shows the Barrett–Joyner–Hanlenda (BJH) pore size distributions.

An automated adsorption apparatus (TriStar) was employed to characterize the surface area and pore size of the activated carbon using N_2 adsorption under 77.35 K. The Brunauer–Emmet–Teller (BET) surface area of the activated carbon was obtained from N_2 adsorption isotherms and pore size distribution was obtained by the Barrett–Joyner–Hanlenda (BJH) and Dollimore–Heal (DH) theory (Table 1). The total pore volume was estimated to be the liquid volume of nitrogen at a relative pressure of about 0.99. The average pore diameter was estimated from the surface area and total pore volume.

According to measurements of adsorption isotherms of the activated carbon (ACPO), we obtained a great specific surface S_{BET} equals to 602.46 m^2/g^{-1}.

The characterization of the distribution of the pore sizes demonstrated the presence of mesopores and micropores. The contact surface related to the mesopores is accessible to the solvated ions of the electrolyte. But for that of micropores, the solvated ions can access only after the deformation of the hydration layer surrounding the ions (Chmiola et al., 2006).

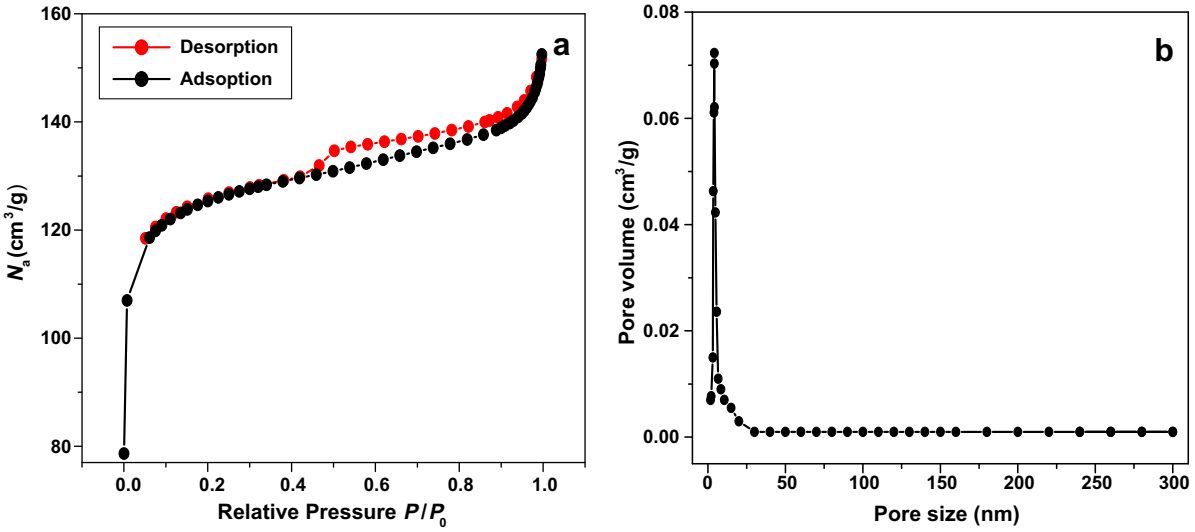

Figure 5 Nitrogen adsorption/desorption isotherm (a) and BJH pore size distributions of the activated carbon (b).

Table 1 Specific surface, pore volume and average pore size of activated carbon.

Specific surface ($m^2\ g^{-1}$)	BJH pore volume ($cm^3\ g^{-1}$)	BJH pore size (nm)	DH pore volume ($cm^3\ g^{-1}$)	DH pore size (nm)
602.46	0,068	4,715	0,079	3,761

3.5. Cyclic Voltammetry study

Cyclic voltammetry (Fig. 6) of ACPO is done at a scan rate of $v = 50$ mV s^{-1} in an aqueous H_2SO_4 (1 M) electrolyte for different potentials namely: 0.15, 0.20, 0.30, 0.4, 0.5, 0.6, 0.65 and 0.7 V/SCE, we observed a good reversibility at the maximum potential of $U = \pm 650$ mV/SCE.

The stored charges at the interface in the EDLC are strongly dependent on the electrode potential as we can see in Fig. 7. We can confirm that the electrode is charged and discharged at a pseudoconstant rate over the complete voltammetric cycle (cycle evolution 1 and 10 cycles for $U = \pm 650$ mV).

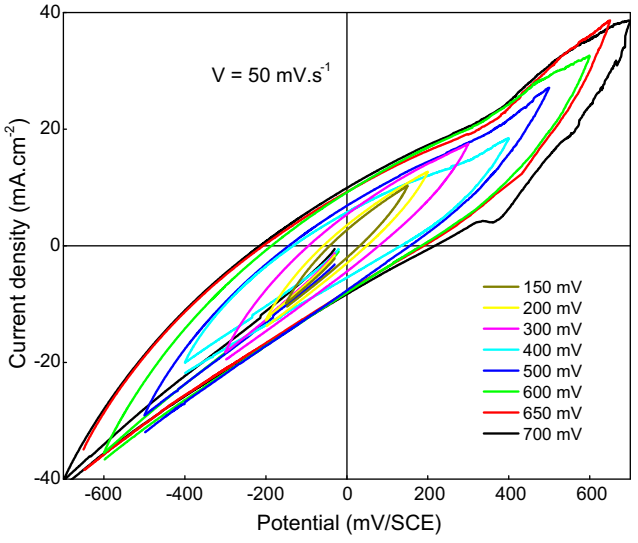

Figure 6 Voltammograms of the activated carbon with various potentials.

3.6. Galvanostatic Chronopotentiometry

Fig. 8 shows the galvanostatic cycling for $U_{max} = \pm 650$ mV/SCE. The current charge and discharge is 30 mA, the charge and discharge time is about 5 s. Fig. 9 shows the cycling evolution for 200 cycles for $I = 30$ mA. During charging and discharging, the various ions found in the solution are H_3O^+ and HSO_4^-. However, the curves of charging/discharging of activated carbon show a nonlinear evolution (the slope variation) of the voltage across the supercapacitor due to dependence of the capacity as a function of tension.

3.7. Electrochemical Impedance Spectroscopy

The analyzed frequency range: 100 kHz (f_{max}) to 10^{-6} kHz (f_{min}) is displayed in Fig. 10. We cannot see a semicircle and the maximum interfacial (surface capacity) and specific capacitances were $C_{s,max} = 3.160$ F cm^{-2} and 158.00 F g^{-1} (Fig. 10b). The results obtained of the activated carbon are displayed in Table 2.

At low frequencies, the entire surface of the activated carbon has all the time to be reached by the ions, it means that the ions can penetrate deeply into the pores and the surface of the electrode has the maximum contribution for optimizing the capacity of the electrochemical double-layer (Harach, 1991).

When the frequency is increased, the capacity decreases and the ion penetration becomes limited with only the interface electrode/solution (Rafik et al., 2007). Fig. 10c represents the

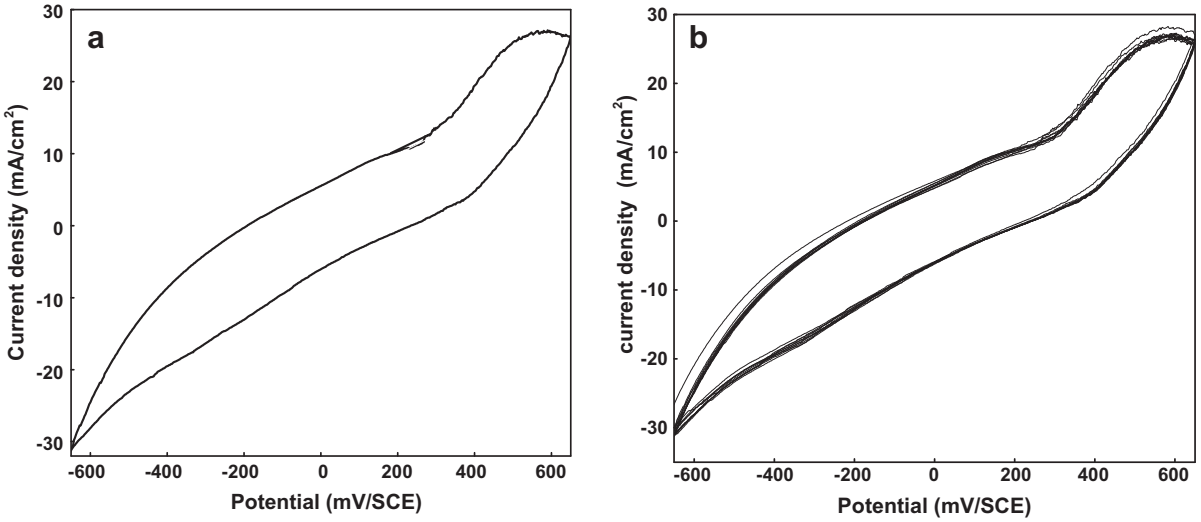

Figure 7 Voltammograms of the AC for $U = \pm 650$ mV/SCE, (a) 1 cycle and (b) 10 cycles.

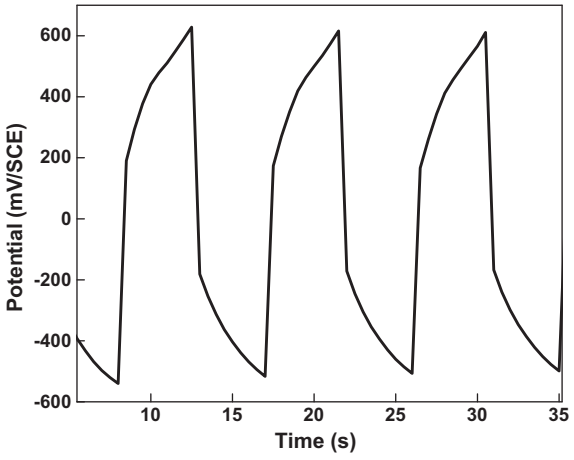

Figure 8 Diagram of charge/discharge of the activated carbon obtained by galvanostatic cycling: $U = \pm 650$ mV/SCE and $I = 30$ mA.

real part of frequency function. The practical results show that the minimal value of the real part is obtained for values of high frequencies. From Fig. 10c, the frequencies beach ranging between 10 kHz and 100 kHz, represents the resistance of the connector industry, that of the contact between the activated carbon and the collector of current and the minimal resistance of the electrolyte (Kötz and Carlen, 2000; Zubieta and Bonert, 1998). These results also show that when the frequency decreases the real part increases. That can be due to the ions which have sufficient time to follow the applied fields and their movements (creating friction) increasing the resistance of the electrolyte. The resulting resistance is denoted as R_{ct} (Resistance of charge transfer). The total series resistance ESR (Equivalent Serial Resistance) of the supercapacitor is ESR = HFR + R_{ct} (Zubieta and Bonert, 1998).

Fig. 11 shows the life of activated carbon supercapacitor. The activated carbon electrode has a highly stable performance up to 10000 cycles. The results obtained of the activated carbon are shown in Table 2.

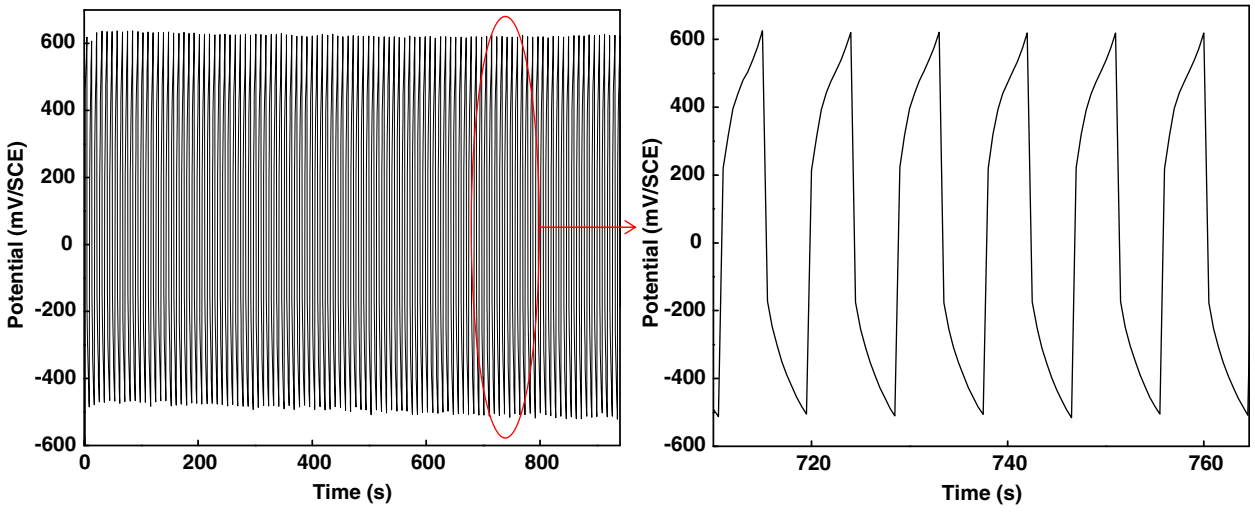

Figure 9 Diagram of charge/discharge of the activated carbon for 200 cycles with $U = \pm 650$ mV/SCE.

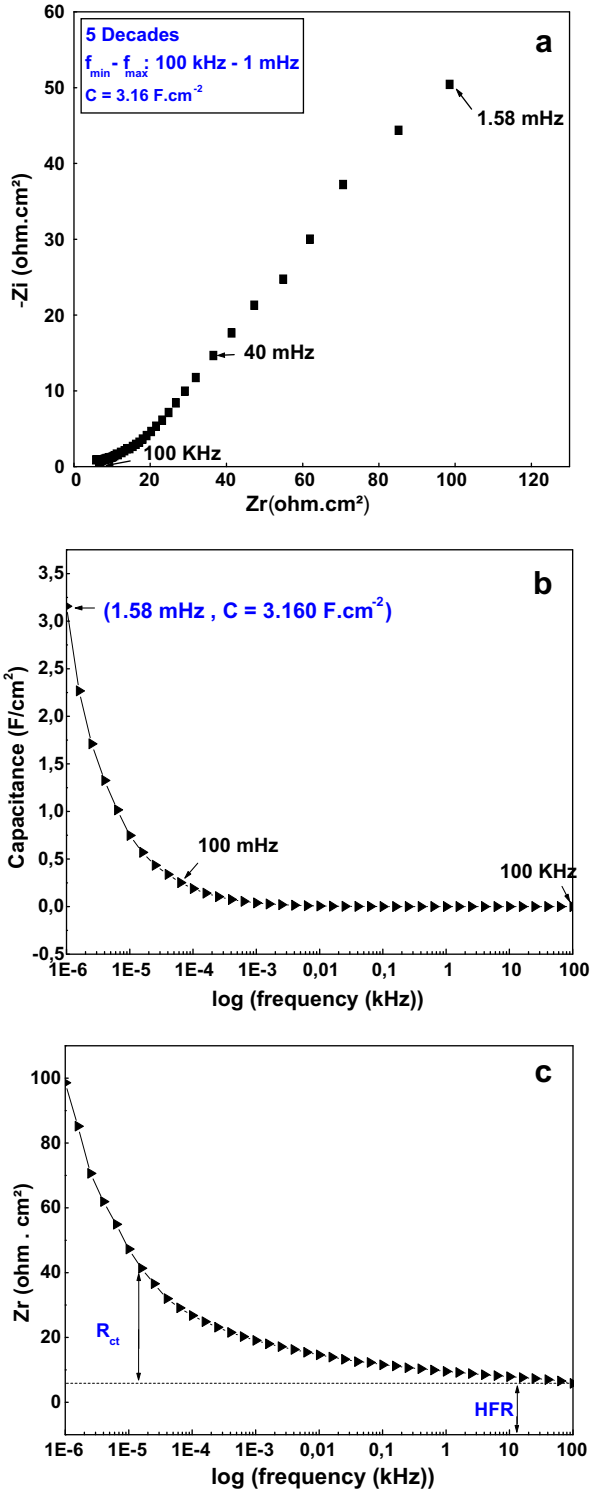

Figure 10 (a) Electrochemical diagram of impedance into the plan of Nyquist (a) and (b) capacity according to the frequency for a surface capacity $C = 3.160$ F cm^{-2} (c) and real part according to the frequency (c).

4. Conclusion

In this work, we realized the synthesis of activated carbon from the biomass of "Posidonia Oceanica" as electrode material for supercapacitor to the electric energy storage.

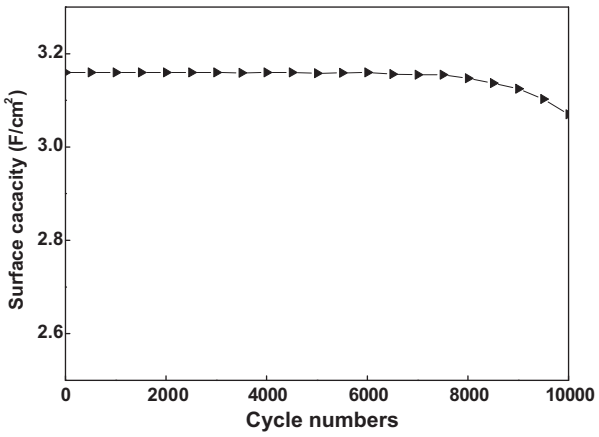

Figure 11 Cycle life of activated carbon supercapacitor.

Table 2 Results obtained of the activated carbon of Posidonia Oceanica.

Surface capacity (F cm^{-2})	Mass capacity (F g^{-1})	Mass energy (W h kg^{-1})	Specific power (kW kg^{-1})
3.16	158	37.08	2.12

The characterizations of the samples by the physicochemical methods, particularly the BET, BJH and DH methods, revealed a great specific surface and the simultaneous existence of mesopores and micropores. The X-ray diffraction analysis revealed a graphite hexagonal structure. SEM images revealed a developed porosity on the entire surface of the layers. The EDS analysis revealed that the activated carbon contains the carbon element in a high atomic percentage of 59.85%. The electrochemical characterizations by the cyclic voltammetry, the galvanostatic chronopotentiometry and the electrochemical impedance spectroscopy demonstrated a capacitive behavior of the system with highly stable performance up to 10,000 cycles. So, the activated carbon from the Posidonia Oceanica can be used as electrodes for supercapacitors.

References

Aravindhan, R., Rao, J.R., Nair, B.U., 2009. J. Hazard. Mater. 162, 688–694.

Balestri, E., Vallerini, F., Lardicci, C., 2006. Coast. Shelf Sci. 66, 30–34.

Burke, A., 2000. J. Power Sources 91, 37–50.

Chmiola, J., Yushin, G., Gogotsi, Y., Portet, C., Simon, P., Tabema, P.L., 2006. Science 313, 1760–1763.

Cocozza, C., Parente, A., Zaccone, C., Mininni, C., Santamaria, P., Miano, T., 2010. Biomass Bioenergy 35, 799–807.

Conway, B.E., 1999. Electrochemical Supercapacitors: Scientific Fundamentals and Technological Applications. Kluwer Academic Publishers, Plenum Press, New York.

Dural, M.U., Cavas, L., Papageorgiou, S.K., Katsaros, F.K., 2010. Chem. Eng. J. 168, 77–85.

Harach, A., 1991. Intercalation électrochimique dans les carbone et le ployacettlene: Approche électrocapillaire. Université de Reims Champagne-Ardenne.

Hazourli, S., Ziati, M., Hazourli, A., Cherifi, M., 2007. Revue des Energies Renouvelables (ICRESD-07 Tlemcen), 187–192.
Huang, Q.H., Wang, X.Y., Li, J., 2006. Electrochim. Acta 52, 1758–1762.
Inagaki, M., Konno, H., Tanaike, O., 2010. J. Power Sources 195, 7880–7903.
Kötz, R., Carlen, M., 2000. Electrochim. Acta 45, 2483–2498.
Lafabrie, C., Pergent, G., Pergent-Martini, C., Capiomont, A., 2007. Environ. Pollut. 148, 688–692.
Ncibi, M.C., Rose, V.J., Mahjoub, B., Marius, C.J., Lambert, J., Ehrhardt, J.J., Bercion, Y., Seffen, M., Gaspard, S., 2009. J. Hazard. Mater. 165, 240–249.
Rafik, F., Gualous, H., Gallay, R., Crausaz, A., Berthon, A., 2007. J. Power Sources 165, 928–934.
Raymundo-Piñero, E., Leroux, F., Béguin, F., 2006. Adv. Mater. 18, 1877–1882.
Rouquerol, F., Rouquerol, J., Sing, K., 1999. Adsorption by Powders & Porous Solids. Principles, Methodology and App. Academic Press, London.
Stimpfling, T., Leroux, F., 2010. Chem. Mater. 22, 974–987.
Zhao, J., Lai, C., Dai, Y., Xie, J., 2007. Mater. Lett. 61, 4639–4642.
Zheng, J.P., 1999. Electrochem. Solid State Lett. 2, 359–361.
Zubieta, L., Bonert, R., 1998. IEEE-IAS 98, 1149–11540.